Nature of Tunable Hole g Factors in Quantum Dots

N. Ares,[1] V. N. Golovach,[1,2,3,4] G. Katsaros,[1,2,5] M. Stoffel,[6] F. Fournel,[7] L. I. Glazman,[8] O. G. Schmidt,[2] and S. De Franceschi[1]

[1]SPSMS, CEA-INAC/UJF-Grenoble 1, 17 Rue des Martyrs, F-38054 Grenoble Cedex 9, France
[2]Institute for Integrative Nanosciences, IFW Dresden, Helmholtzstrasse 20, D-01069 Dresden, Germany
[3]IKERBASQUE, Basque Foundation for Science, E-48011 Bilbao, Spain
[4]Centro de Física de Materiales (CFM-MPC), Centro Mixto CSIC-UPV/EHU, Manuel de Lardizabal 5, E-20018 San Sebastián, Spain
[5]Johannes Kepler University, Institute of Semiconductor and Solid State Physics, Altenbergerstrasse 69, 4040 Linz, Austria
[6]Université de Lorraine, Institut Jean Lamour, UMR CNRS 7198, Nancy-Université, BP 239, F-54506 Vandoeuvre-les-Nancy, France
[7]CEA, LETI, MINATEC, 17 Rue des Martyrs, F-38054 Grenoble Cedex 9, France
[8]Department of Physics, Yale University, New Haven, Connecticut 06520, USA

(Received 24 July 2012; revised manuscript received 12 October 2012; published 23 January 2013)

We report an electric-field-induced giant modulation of the hole g factor in SiGe nanocrystals. The observed effect is ascribed to a so-far overlooked contribution to the g factor that stems from the mixing between heavy- and light-hole wave functions. We show that the relative displacement between the confined heavy- and light-hole states, occurring upon application of the electric field, alters their mixing strength leading to a strong nonmonotonic modulation of the g factor.

DOI: 10.1103/PhysRevLett.110.046602 PACS numbers: 72.25.Dc, 71.70.Ej, 73.23.Hk, 73.63.Kv

In the past decade, a great effort has been devoted to the realization of spin qubits in semiconductors [1,2]. Spin manipulation was achieved through different approaches: magnetic-field-driven electron spin resonance [3], electric-dipole spin resonance [4–6], and fast control of the exchange coupling [7]. Another possibility for electric-field spin manipulation is the g-tensor modulation resonance, which has been used on ensembles of spins in two-dimensional (2D) electron systems [8,9]. This technique relies on anisotropic and electrically tunable g factors. Recently, several experiments have addressed the g-factor modulation by means of external electric fields [10,11], and different mechanisms were evoked to explain the observed g-factor tunability, such as compositional gradients [10] and quenching of the angular momentum [11,12]. Here we report the experimental observation of an exceptionally large and nonmonotonic electric-field modulation of the hole g factor in SiGe quantum dots (QDs). To interpret this finding we have to invoke a new mechanism that applies to hole-type low-dimensional systems. This mechanism relies on the existence of an important, yet overlooked correction term in the g factor whose magnitude depends on the mixing of heavy and light holes. We show that in SiGe self-assembled QDs an electric field applied along the growth axis can be used to efficiently alter this mixing and produce large variations in the hole g factor.

Our SiGe QDs were grown by molecular-beam epitaxy on a silicon-on-insulator substrate. The Stranski-Krastanow growth mode was tuned to yield dome-shaped QDs with height $w = 20$ nm and base diameter $d = 80$ nm. A sketch of the device is shown in Fig. 1(a). The QD is contacted by two 20-nm-thick Al electrodes, acting as source and drain leads. A Cr-Au gate electrode is fabricated on top of the QD with a 6-nm-thick hafnia interlayer deposited by atomic-layer deposition. This top gate, together with the degenerately doped Si back gate, allows a perpendicular electric field to be applied while maintaining a constant number of holes in the SiGe QD. To a first approximation, we dispense with the screening effect of the source and drain electrodes and assume the electric field to be homogeneous in space.

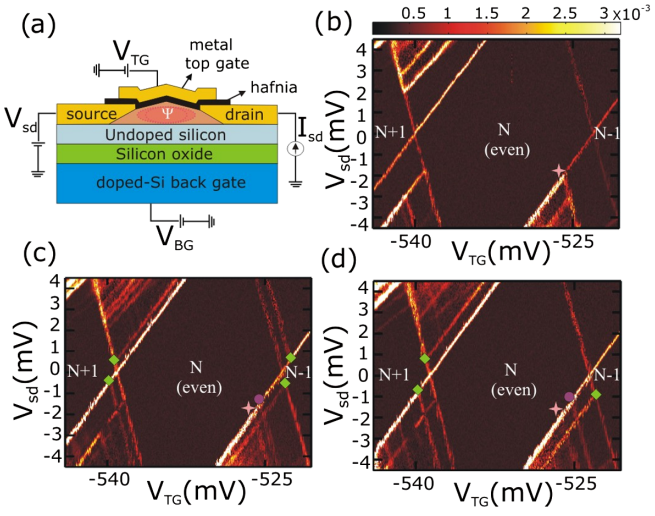

FIG. 1 (color online). (a) Schematic cross section of a SiGe QD device. (b)–(d) Color plot of $dI_{sd}/dV_{sd}(V_{TG}, V_{sd})$ for $B_z =$ 70 mT, 3 T, and 5 T, respectively ($V_{BG} = 0$). The lines indicated by rhombi correspond to the onset of tunneling via Zeeman-split levels for $N - 1$ and $N + 1$ holes on the QD. The lines indicated by a star and by a circle correspond to singlet-triplet excitations for N holes.

Measurements of the g factor were performed using single-hole tunneling spectroscopy. A typical differential conductance (dI_{sd}/dV_{sd}) measurement as a function of top-gate voltage (V_{TG}) and source-drain bias voltage (V_{sd}) is shown in Fig. 1(b). All measurements reported here were done in a ^{3}He refrigerator with a base temperature of 250 mK. In order to suppress the superconductivity of the leads, a small magnetic field, $B_z = 70$ mT, was applied along the z axis, i.e., perpendicular to the (x, y) growth plane. Diamond-shaped regions, where the current vanishes due to Coulomb blockade, can be clearly observed in Fig. 1(b). The charging energy is about 10 meV. Outside the diamonds, additional lines denoting transport through excited orbital states can be observed. Figs. 1(c) and 1(d) show the same Coulomb-blockade regime for $B_z = 3$ T and $B_z = 5$ T, respectively. The magnetic field causes a splitting of the diamond edges as indicated by green rhombi. This splitting follows from the lifting of Kramers degeneracy in the ground states associated with the side diamonds. We thus conclude that the central diamond corresponds to an even number, N, of confined holes [1]. The Zeeman splitting is given by $E_Z = g_\perp \mu_B B_z$, where μ_B is the Bohr magneton and $g_\perp$ is the absolute value of the g factor along z. From the splitting of the N-hole diamond edges we extract $g_\perp = (3.0 \pm 0.4)$ and $g_\perp = (2.8 \pm 0.4)$ for the $N-1$ and the $N+1$ ground states, respectively. The line indicated by a star in Fig. 1(b) is due to the spin-triplet excited state for N holes on the QD. We measure a 2 meV singlet-triplet energy in this particular QD, which is an order of magnitude larger than for electrons in Si/SiGe heterostructures [13]. We note that large singlet-triplet excitation energies are particularly desirable for the observation of spin blockade in double-dot experiments [14]. Upon increasing B_z, the line denoted by a star splits as shown by the emergence of a second parallel line, denoted by a circle, that shifts away proportionally to B_z [see Figs. 1(c) and 1(d)]. This behavior corresponds to the Zeeman splitting of the excited spin-triplet state [1] with $g_\perp = (2.8 \pm 0.4)$. Hereafter, we will concentrate on g-factor measurements in spin-1/2 ground states.

Our dual-gate devices allow us to measure the dependence of the g factor on a perpendicular electric field, F, at a constant number of holes. The principle of such a measurement is illustrated in Fig. 2(a). The Zeeman splitting is given by the distance between the blue and the red circles along V_{BG}, multiplied by a calibration factor α. The latter is obtained by dividing V_{sd} by the distance between the green and the red circles. In order to investigate the F dependence of the g factor, we set $B_z = 4$ T, $V_{sd} = 2.6$ mV, and sweep V_{BG} for different V_{TG}. The data is shown in Fig. 2(b) and the extracted g factors are displayed in Fig. 2(c). We observe an exceptionally large g-factor modulation ($\delta g/g \sim 1$) denoting a strong effect of the applied F. The g factor increases slowly to a maximum

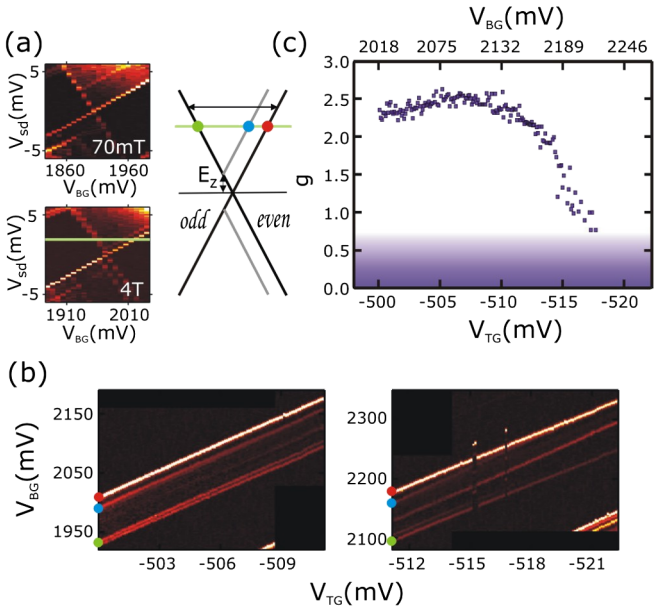

FIG. 2 (color online). (a) Left: Color plots of $dI_{sd}/dV_{sd}(V_{\mathrm{BG}}, V_{sd})$ for $B = 70$ mT and 4 T. At 4 T the Zeeman splitting is clearly visible. Right: Corresponding schematic diagram illustrating the measurement principle to extract the Zeeman energy splitting (and hence the g factor) from gate-voltage sweeps at constant V_{sd} (see the horizontal green line). (b) Color plots of $dI_{sd}/dV_{sd}(V_{\mathrm{BG}}, V_{\mathrm{TG}})$ for a fixed $V_{sd} = 2.6$ mV. These data sets demonstrate the modulation of $g_\perp$ by the top and back gates. (c) $g_\perp(V_{\mathrm{BG}}, V_{\mathrm{TG}})$ as extracted from (b). Below $g_\perp \approx 0.75$ the Zeeman splitting cannot be resolved any more due to the finite broadening of the tunneling resonances.

value of 2.6 and then drops rapidly till the Zeeman splitting can no longer be resolved. Comparably large g-factor variations have been observed in other similar measurements (see Supplemental Material [15]).

In order to uncover the origin of this unusual behavior, we modelled the QD electronic states in terms of heavy-hole (HH) and light-hole (LH) subbands. Given the relatively large anisotropy of dome-shaped QDs, we initially considered the 2D limit resulting from confinement along the growth axis. Confinement and strain lift the fourfold degeneracy of the valence band at the Γ point. The topmost subband has HH character and its in-plane dispersion relation is described by the effective 2D Hamiltonian

$$H_{\mathrm{eff}} = \frac{1}{2m_\parallel}(k_x^2 + k_y^2) + \frac{1}{2} g_\parallel \mu_B (\sigma_x B_x + \sigma_y B_y) - \frac{1}{2} g_\perp \mu_B \sigma_z B_z + U(x, y), \quad (1)$$

where k_x and k_y are the in-plane momentum operators, $m_\parallel = m/(\gamma_1 + \gamma_2)$ is the in-plane effective mass [16], $g_\parallel = 3q$ and $g_\perp = 6\kappa + \frac{27}{2} q$ are, respectively, the in-plane and transverse g factors [16,17], $\boldsymbol{\sigma}$ are the Pauli matrices in the pseudospin space [18], and $U(x, y)$ is the in-plane confining potential in the QD. We use standard notations

for the Luttinger parameters γ_1, γ_2, γ_3, κ, and q [20]. Since $q \ll \kappa$, it is appropriate to assume $g_\perp \approx 6\kappa$ [21].

First, we consider the possibility that the observed g-factor modulation arises from a compositional gradient. This mechanism was exploited in $Al_xGa_{1-x}As$ quantum wells to implement electrical control of electron spins [8,9]. In Stranski-Krastanow QDs, Si and Ge form a $Si_{1-x}Ge_x$ alloy in which x increases monotonically with z, being zero at the base ($z = -w$) and approaching unity at the apex ($z = 0$) of the QD [22]. Since $\kappa_{Si} = -0.42$ and $\kappa_{Ge} = 3.41$, one would expect that $g_\perp$ increases with F following a vertical shift of the HH wave function towards the apex.

To find an upper bound for the g-factor variation resulting from the compositional gradient, we take the steepest dependence reported for the Ge content across the QD [22],

$$\mathsf{x}(z) = \mathsf{x}_{\max}\sqrt{1 + \frac{z}{w}}, \qquad -w < z < 0. \tag{2}$$

To account for the existing uniaxial strain, we assume that the in-plane lattice constant $a_\parallel$ increases linearly from 5.47 Å at the base to 5.59 Å at the apex [22]. The resulting valence-band profiles $E_v(z)$ for all types of holes are calculated using interpolation schemes devised for SiGe [23,24] (see inset of Fig. 3). The HH ground state is thus confined to a triangular potential well arising from the compositional gradient. An electric field applied along z adds a term $-eFz$ to $E_v(z)$. For a given F, the HH wave function $\psi(z)$ is obtained by solving the Schrödinger equation numerically. The HH g factor is found as a weighted average

$$g_\perp \approx 6\langle\kappa\rangle = 6\int \kappa(\mathsf{x}(z))|\psi(z)|^2 dz, \tag{3}$$

where $\kappa(\mathsf{x})$ is obtained as described in Ref. [25]. The resulting $g_\perp(F)$ dependence is shown in Fig. 3. We distinguish two regimes: that of a strongly asymmetric (triangular) potential well and that of a symmetric potential well. The modulation of the g factor is largest in the latter regime (see dotted line), where $dg_\perp/dF \approx 0.41$ m/MV. While the magnitude of the modulation is close to what is observed in the experiment, the sign of $dg_\perp/dF$ is opposite. We conclude that the compositional gradient cannot explain our data. Therefore, from now on, we shall discard this mechanism and assume the Ge content to be constant within the QD.

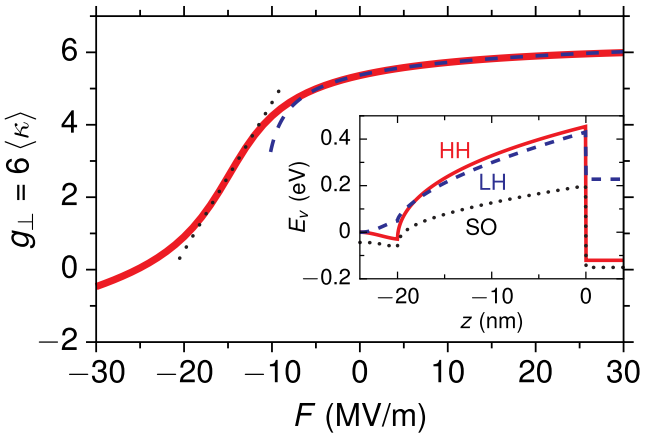

FIG. 3 (color online). Expected $g_\perp(F)$ dependence for a SiGe QD with strong compositional gradient. The numerical result (solid line) has two regimes: the dashed line shows a fit to the expression $\langle\kappa\rangle = \kappa_\infty - \Delta\kappa(1 + F/F_{\text{intr}})^{-1/3}$, derived for a triangular potential well with an intrinsic field F_{intr} for $z < 0$ and an infinite barrier for $z > 0$; the dotted line is a fit to a linear dependence, obtained for a symmetric potential well. In the latter regime, $g_\perp$ is most sensitive to F, with $dg_\perp/dF = 0.41$ m/MV. At large negative F, the wave function is pushed into the Si-rich region, where $g_\perp < 0$. Inset: Energy profiles for the heavy-hole (HH), light-hole (LH), and split-off (SO) bands as calculated from Eq. (2) with $x_{\max} = 0.8$. We set $x = 0$ for $z < -20$ nm to account for the Si substrate, and $x = 0$ for $z > 0$ to account for the existence of a strained, few-nm-thick Si capping layer.

We revisit the derivation of Eq. (1), starting from the 4×4 Luttinger Hamiltonian, which, in the 2D limit, separates into 2×2 blocks: two diagonal blocks, H_{hh} and H_{ll}, corresponding to the HH and the LH sector, respectively; two off-diagonal blocks, H_{LH} and H_{HL}, connecting the HH sector to the LH sector (see Supplemental Material [15]). To leading order in $w/d \ll 1$, the HH and LH sectors are connected by the off-diagonal mixing blocks [19]

$$H_{hl} = (H_{lh})^\dagger = i\frac{\sqrt{3}\gamma_3}{m}(k_x\sigma_y + k_y\sigma_x)k_z, \tag{4}$$

where k_x and k_y are 2D versions of momentum operators (insensitive to in-plane magnetic fields), $k_z \equiv -i\hbar\partial/\partial z$, and σ_x and σ_y are the Pauli matrices in a pseudospin space [19].

The mixing blocks in Eq. (4) are proportional to k_z. In spite of the fact that k_z averages to zero for each type of hole separately, it cannot be discarded in Eq. (4), because matrix elements of the type $\langle\psi_h|k_z|\psi_l\rangle$ are, in general, nonzero and scale as $1/w$ for $w \to 0$. Here, $\psi_h(z)$ and $\psi_l(z)$ obey two separate Schrödinger equations, for heavy and light holes, respectively (see below). This observation allows us to anticipate that in second-order perturbation theory the mixing blocks lead to an energy correction containing $H_{hl}H_{lh} \propto k_z^2$ in the numerator and $H_{ll} - H_{hh} \propto k_z^2$ in the denominator. This correction does not vanish in the 2D limit ($k_z \to \infty$). At the same time, the correction to the wave function vanishes as $k_\parallel/k_z \sim w/d$.

Using second-order perturbation theory, we recover Eq. (1) for the topmost hole subband. Yet, at the leading (zeroth) order in $w/d \ll 1$, we obtain the following modified expressions for the effective mass and the perpendicular g factor,

$$m_\parallel = \frac{m}{\gamma_1 + \gamma_2 - \gamma_h}, \qquad g_\perp = 6\kappa + \frac{27}{2}q - 2\gamma_h. \tag{5}$$

The in-plane g factor remains unchanged ($g_\parallel = 3q$) at this order. In Eq. (5), γ_h is a dimensionless parameter sensitive to the form of the confinement along z,

$$\gamma_h = \frac{6\gamma_3^2}{m}\sum_n \frac{|\langle \psi_n^l | k_z | \psi_1^h \rangle|^2}{E_n^l - E_1^h}. \quad (6)$$

Here, the sum runs over the LH subbands and the wave functions $\psi_n^{h\,(l)}(z)$ and energies $E_n^{h\,(l)}$ obey

$$\left[\frac{k_z^2}{2m_\perp^{h\,(l)}} + V_{h\,(l)}(z)\right]\psi_n^{h\,(l)}(z) = E_n^{h\,(l)}\psi_n^{h\,(l)}(z), \quad (7)$$

where $m_\perp^{h\,(l)} = m/(\gamma_1 \mp 2\gamma_2)$ and $V_{h\,(l)}(z)$ is the confining potential seen by the heavy (light) hole. The electric field contributes to $V_{h\,(l)}(z)$ with the term $-Fz$ [26].

When $V_h(z)$ and $V_l(z)$ are infinite square wells, an analytical derivation yields

$$\gamma_h = \frac{12\gamma_3^2}{\gamma_1 + 2\gamma_2}\left[\frac{1}{1-\beta} - \frac{4\sqrt{\beta}}{\pi(1-\beta)^2}\cot\left(\frac{\pi}{2}\sqrt{\beta}\right)\right], \quad (8)$$

where $\beta = m_\perp^l/m_\perp^h + \delta E_{001}/E_1^l$, with $\delta E_{001} \equiv V_h - V_l$ being the splitting of the valence band due to uniaxial strain and $E_1^l = \pi^2\hbar^2/2m_\perp^l w^2$. Notably, one has $\psi_n^h(z) = \psi_n^l(z)$ in this case, because the masses $m_\perp^h$ and $m_\perp^l$ drop out of the expressions for the wave functions. An electric field causes $\psi_n^h(z)$ and $\psi_n^l(z)$ to shift relative to each other, because of the different effective masses, $m_\perp^h \neq m_\perp^l$. Although γ_h can only be numerically computed, its qualitative F-dependence can be inferred from Eq. (6). The $n = 1$ term dominates the sum due to its smallest energy denominator. For a square-well potential, however, this term vanishes by symmetry. As a result, the symmetric point $F = 0$ corresponds to a minimum in $\gamma_h(F)$, since $E_n^l > E_1^h$. Away from $F = 0$, γ_h increases quadratically, $\gamma_h \propto F^2$, up to the point where the electric field is strong enough to shift the HH wave function ($eFw \simeq E_2^h - E_1^h$). Then, γ_h increases roughly linearly up to the point where the LH wave functions begin to shift ($eFw \simeq E_2^l - E_1^l$). Upon further increasing F, γ_h increases weakly and saturates to a constant. We remark that $g_\perp$ is modified by γ_h even at $k_\parallel = 0$, despite the absence of HH-LH mixing at $k_\parallel = 0$. In fact, since $g_\perp$ is sensitive to in-plane orbital motion [27], even a small B_z translates to $k_\parallel \neq 0$, leading to HH-LH mixing.

Our result in Eq. (5) represents the zeroth-order term in the expansion $g = g^{(0)} + g^{(2)} + \cdots$, where $g^{(2)} \propto (w/d)^2$ is the subleading-order term. Unlike the main term, the correction $g^{(2)}$ is sensitive to the in-plane confining potential $U(x, y)$ and it originates from the HH-LH interference terms in the wave function. In Fig. 4, we fit the experimental data using only the leading, zeroth-order term. The HH and LH wave functions, $\psi_1^h(z)$ and $\psi_1^l(z)$, shift upon application of the electric field. The transition from square well (central inset) to triangular well (highest insets) occurs in two steps. First, $\psi_1^h(z)$ shifts by $\delta z \sim w$, while $\psi_1^l(z)$ remains nearly unaffected (lowest insets). Then, $\psi_1^l(z)$ shifts as well (highest insets). At even larger F (not shown) $g_\perp$ saturates to $g_\perp \approx 0.6$. The calculated $g_\perp(F)$ dependence, taking into account γ_h, qualitatively reproduces the experimental data. We have also verified that the inclusion of an electric-field gradient into our model (as a result of screening by source and drain electrodes) improves the agreement between theory and experiment, see dashed line in Fig. 4.

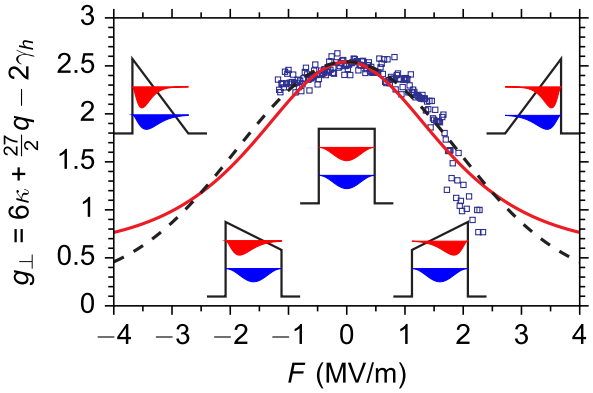

FIG. 4 (color online). The $g_\perp(F)$ dependence according to Eq. (5) (solid line) superimposed on the experimental data (squares) of Fig. 2(c). Since the variations in V_{BG} and V_{TG} are proportional to each other, we take $F = aV_{TG} + b$, with fitting parameters a and b. The dashed line is an improved fit obtained with a model that allows for a field gradient across the SiGe nanocrystal (such a gradient is expected as a screening effect of the source and drain electrodes). For $z \in [-w, 0]$, we assume an electrostatic potential of the form $V(z) = -cF(z + w/2)^2 - Fz$, where c is a fit parameter. Insets: Schematics of the HH (red) and LH (blue) wave functions at different F. At finite, intermediate fields (lowest insets) the two wave functions are shifted relative to each other resulting in the largest $|dg_\perp/dF|$.

Finally, we remark that the correct 2D limit of the Luttinger Hamiltonian has been largely overlooked. Although our main result in Eq. (5) bears some relation to earlier works [28], the relation of $m_\parallel$ and $g_\perp$ to an additional parameter γ_h and the fact that γ_h is sensitive to F have been missing from the general knowledge of 2D hole systems.

In conclusion, we showed that an external electric field can strongly modulate the perpendicular hole g factor in SiGe QDs. By a detailed analysis, we ruled out the compositional-gradient mechanism as the origin of this electric-field effect. By analyzing the Luttinger Hamiltonian in the 2D limit, we found a new correction term γ_h which had not been considered before in the literature. This new term, which corrects the "standard" expression for the HH g factor, reflects the effect of a perpendicular magnetic field on the orbital motion, and it is ultimately related to the atomistic spin-orbit coupling of the valence band.

We acknowledge financial support from the Nanosciences Foundation (Grenoble, France), DOE under

Contract No. DEFG02-08ER46482 (Yale), the Agence Nationale de la Recherche, and the European Starting Grant. G. K. acknowledges support from the European Commission via a Marie Curie Carrer Integration Grant and the FWF for a Lise-Meitner Fellowship.

[1] R. Hanson, L. P. Kouwenhoven, J. R. Petta, S. Tarucha, and L. M. K. Vandersypen, Rev. Mod. Phys. **79**, 1217 (2007).
[2] D. Loss and D. P. DiVincenzo, Phys. Rev. A **57**, 120 (1998).
[3] F. H. L. Koppens, C. Buizert, K. J. Tielrooij, I. T. Vink, K. C. Nowack, T. Meunier, L. P. Kouwenhoven, and L. M. K. Vandersypen, Nature (London) **442**, 766 (2006).
[4] K. C. Nowack, F. H. L. Koppens, Yu. V. Nazarov, and L. M. K. Vandersypen, Science **318**, 1430 (2007).
[5] S. Nadj-Perge, S. M. Frolov, E. P. A. M. Bakkers, and L. P. Kouwenhoven, Nature (London) **468**, 1084 (2010).
[6] V. N. Golovach, M. Borhani, and D. Loss, Phys. Rev. B **74**, 165319 (2006).
[7] J. R. Petta, A. C. Johnson, J. M. Taylor, E. A. Laird, A. Yacoby, M. D. Lukin, C. M. Marcus, M. P. Hanson, and A. C. Gossard, Science **309**, 2180 (2005).
[8] Y. Kato, R. C. Myers, D. C. Driscoll, A. C. Gossard, J. Levy, and D. D. Awschalom, Science **299**, 1201 (2003).
[9] G. Salis, Y. Kato, K. Ensslin, D. C. Driscoll, A. C. Gossard, and D. D. Awschalom, Nature (London) **414**, 619 (2001).
[10] R. S. Deacon, Y. Kanai, S. Takahashi, A. Oiwa, K. Yoshida, K. Shibata, K. Hirakawa, Y. Tokura, and S. Tarucha, Phys. Rev. B **84**, 041302 (2011).
[11] V. Jovanov, T. Eissfeller, S. Kapfinger, E. C. Clark, F. Klotz, M. Bichler, J. G. Keizer, P. M. Koenraad, G. Abstreiter, and J. J. Finley, Phys. Rev. B **83**, 161303 (2011).
[12] C. E. Pryor and M. E. Flatté, Phys. Rev. Lett. **96**, 026804 (2006).
[13] N. Shaji, C. B. Simmons, M. Thalakulam, L. J. Klein, H. Qin, H. Luo, D. E. Savage, M. G. Lagally, A. J. Rimberg, R. Joynt, M. Friesen, R. Blick, S. N. Coppersmith, and M. A. Eriksson, Nat. Phys. **4**, 540 (2008).
[14] K. Ono, D. G. Austing, Y. Tokura, and S. Tarucha, Science **297**, 1313 (2002).
[15] See Supplemental Material at http://link.aps.org/supplemental/10.1103/PhysRevLett.110.046602 for additional experimental data and a detailed derivation of γ_h.
[16] R. Winkler, *Spin-Orbit Coupling Effects in Two-Dimensional Electron and Hole Systems* (Springer, New York, 2003).
[17] H. W. van Kesteren, E. C. Cosman, W. A. J. A. van der Poel, and C. T. Foxon, Phys. Rev. B **41**, 5283 (1990).
[18] We choose the pseudospin basis as in Ref. [19]; namely, $|\uparrow\rangle_h = |3/2, -3/2\rangle$ and $|\downarrow\rangle_h = |3/2, +3/2\rangle$.
[19] G. Katsaros, V. N. Golovach, P. Spathis, N. Ares, M. Stoffel, F. Fournel, O. G. Schmidt, L. I. Glazman, and S. De Franceschi, Phys. Rev. Lett. **107**, 246601 (2011).
[20] J. M. Luttinger, Phys. Rev. **102**, 1030 (1956).
[21] The minus sign in front of $\frac{1}{2}g_\perp$ in Eq. (1) is introduced for the convenience of having $g_\perp$ positive for Ge.
[22] T. U. Schülli, M. Stoffel, A. Hesse, J. Stangl, R. T. Lechner, E. Wintersberger, M. Sztucki, T. H. Metzger, O. G. Schmidt, and G. Bauer, Phys. Rev. B **71**, 035326 (2005).
[23] C. G. Van de Walle and R. M. Martin, Phys. Rev. B **34**, 5621 (1986).
[24] M. M. Rieger and P. Vogl, Phys. Rev. B **48**, 14276 (1993).
[25] R. Winkler, M. Merkler, T. Darnhofer, and U. Rössler, Phys. Rev. B **53**, 10858 (1996).
[26] In piezoelectric materials (not in SiGe), the application of an electric field may change the strain distribution inside the nanocrystal, giving rise to additional terms in $V_h(z)$ and $V_l(z)$ proportional to the electric field.
[27] K. A. Matveev, L. I. Glazman, and A. I. Larkin, Phys. Rev. Lett. **85**, 2789 (2000).
[28] D'yakonov and Khaetskii [29] studied the Luttinger Hamiltonian in an infinite square well and used the spherical approximation ($\gamma_2 = \gamma_3$). They derived an expression for $m_\parallel$ that agrees with our result in the appropriate limit. We also verified that Eqs. (5) and (6) can be obtained from a general $\boldsymbol{k}\cdot\boldsymbol{p}$ approach [30,31] after a lengthy calculation.
[29] M. I. D'yakonov and A. V. Khaetskii, Zh. Eksp. Teor. Fiz. **82**, 1584 (1982) [Sov. Phys. JETP **55**, 917 (1982).
[30] L. Roth, B. Lax, and S. Zwerdling, Phys. Rev. **114**, 90 (1959).
[31] A. A. Kiselev, E. L. Ivchenko, and U. Rössler, Phys. Rev. B **58**, 16353 (1998).